Design Parameters and Performance Limits for a Nanomolding-Nanoassembly Self-Contained Manufacturing Platform.

Colin Kakama.
kakamatech@gmail.com
Independent Researcher.

Abstract.

Mechanosynthetic nanofactory architectures are computationally well-supported but demand angstrom-level atomically precise fabrication as a prerequisite, a capability that remains practically inaccessible for first-generation physical implementation. This paper proposes the nanomolding-nanoassembly (NMNA) nanofactory as a credible intermediate pathway: a self-contained manufacturing platform with 100 nm characteristic dimensions that fabricates nanoscale mechanical components via thermoplastic nanomolding and assembles them deterministically using nanoscale mechanical proxies, without requiring atomically precise construction.

The framework is developed across four primary areas. First, material selection criteria are derived from first principles and biodegradable polymers are adopted as the V1 primary material, with stiffness limitations addressed through geometric stiffening and stimulation-induced transient rigidity strategies. Second, a minimum viable part library for dexterous nanoassembly is defined. Third, surface force management is treated as a first-order design constraint, with stiction and kinetic friction at the 10-50 nm scale analyzed and mitigation strategies proposed. Fourth, a nanoshedding safety framework is established, requiring that all nano-products entering biological or ecological environments be fabricated from biodegradable materials with defined degradation pathways.

The paper concludes with a structured experimental program organized into three tiers ordered to resolve the framework's primary unknowns in logical dependency order. The NMNA architecture does not replicate the full capability of mechanosynthetic systems, but it establishes an experimentally approachable foundation from which productive nanomechanical manufacturing can be pursued.

1. Introduction

The long-standing vision of the molecular nanotechnology (MNT) field has been the creation of nanometer-scale mechanical systems capable of transformative capabilities: materials engineered with atomically precise structures, medical nanorobots able to manipulate cellular processes beyond the reach of conventional small-molecule or biologic therapies, and generalised nanoassemblers capable of fabricating a wide range of macro-scale products from abundant feedstocks with minimal waste and potentially recursive self-improvement.

In most proposals, such systems rely on molecular-scale mechanical components with features approaching atomic dimensions. Their construction therefore demands deterministic atom-by-atom fabrication using mechanochemical tooltips[1] capable of precise bond placement. However, although substantial theoretical and computational progress has been made in modeling these architectures, experimental realization of single atom 3d positioning and molecular manufacturing has been scarce. Practical bottlenecks include extreme vibration isolation requirements, stringent ultra-high vacuum (UHV) environments, limited throughput of serial atom placement, and many other non-trivial bootstrapping challenges for constructing the first generation of atomically precise machinery.

This work recognizes this experimental immaturity and proposes an alternative pathway to creating productive nanomechanical systems that does not require angstrom-level atomically precise manufacturing (APM). Instead, it explores a framework in which nanoscale mechanical components can be fabricated through nanomolding processes[2][22] followed by deterministic assembly using rigid nanoscale parts and specialized mechanical tools.

This paper develops the concept of the nanomolding-nanoassembly(NMNA) nanofactory. A self contained device measuring no more than $100nm^3$, that molds feedstock into nanoparts and assembles them into desirable 3D structures capable of achieving a substantial subset of the functional promises associated with mechanosynthetic architectures[3].

A note on the nature of this contribution. This paper is a design specification, not an experimental report. It establishes the parameter space within which a first-generation NMNA nanofactory must operate: the material constraints, the minimum viable part library, the surface force management requirements, and the stiffness augmentation strategies available to polymer-based components. No fabrication has been attempted; no functional demonstration is reported. The value of the framework lies in its function as an engineering target. Readers should evaluate the contribution accordingly: not as a proof that the NMNA architecture works, but as a rigorous account of what would have to be demonstrated for it to work, and why that demonstration is now tractable.

2. Conceptual Architecture of a NMNA nanofactory

The nanomolding–nanoassembly (NMNA) nanofactory operates according to a two-stage manufacturing paradigm (Fig. 1). First, material is introduced into engineered nanoscale cavities, where it undergoes controlled molding to form discrete mechanical components. Second, the molded parts are extracted by dexterous nanoscale machines and deterministically joined to previously fabricated components, progressively building higher-order structures until a target architecture is achieved.

The fabrication stage draws from principles established in semiconductor manufacturing, particularly nanoimprint lithography[4], in which viscous or thermally softened materials are driven into nanostructured molds and subsequently solidified to preserve geometry. In the NMNA framework, this process is adapted from planar pattern transfer to the production of three-dimensional nanoscale mechanical elements.

The assembly stage is carried out by mechanically functionalized nanoparticles whose geometries and roles emulate those of the molecular scale nanomachines most prominently articulated by K.Eric Drexler[5].

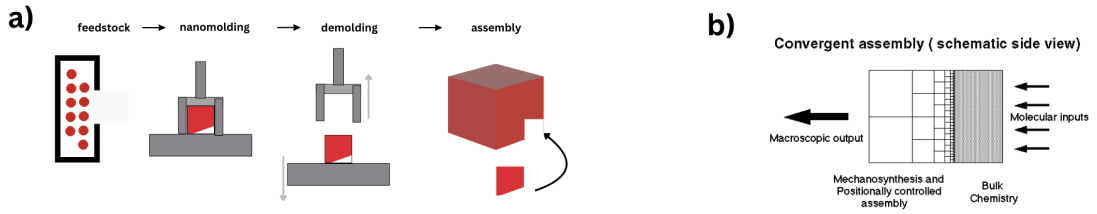

Figure 1. Illustration of a nanomolding-nanoassembly architecture and convergent assembly. a) Feedstock being molded and assembled into a macroproduct b) An illustration of hierarchical convergent assembly from molecules to macro products in a mechanosynthetic nanofactory[21].

The NMNA nanofactory is volumetrically constrained to 100 nm³. This is motivated by a downstream deployment target: intracellular operation within living cells without inducing cell death. Experimental work on nanoneedle-based intracellular probes has established a practical upper diameter limit of approximately 200 nm for non-lethal membrane penetration, with probes below this threshold preserving cell viability across mammalian cell types including HeLa and mouse fibroblasts [29]. A device fitting within a 100 nm³ envelope (well below this biological compatibility threshold) is therefore sized to remain viable as a future intracellular agent[30]. The V1 NMNA nanofactory is not designed for immediate intracellular deployment; it is sized from the outset to be compatible with that trajectory. Demonstrating productive nanomechanics at this scale constitutes the foundational step toward nanomechanical systems that can operate within the intracellular environment.

3. Nanopart Fabrication via Nanomolding

3.1 Principles of Nanomolding

Nanomolding requires application of a driving force to a moldable material so it can fill a mold cavity and upon setting, either by cooling or chemical means, a hardened structure in the geometry of the cavity can be recovered. (Fig 2) while achieving up to sub 10nm feature sizes in some products[22]

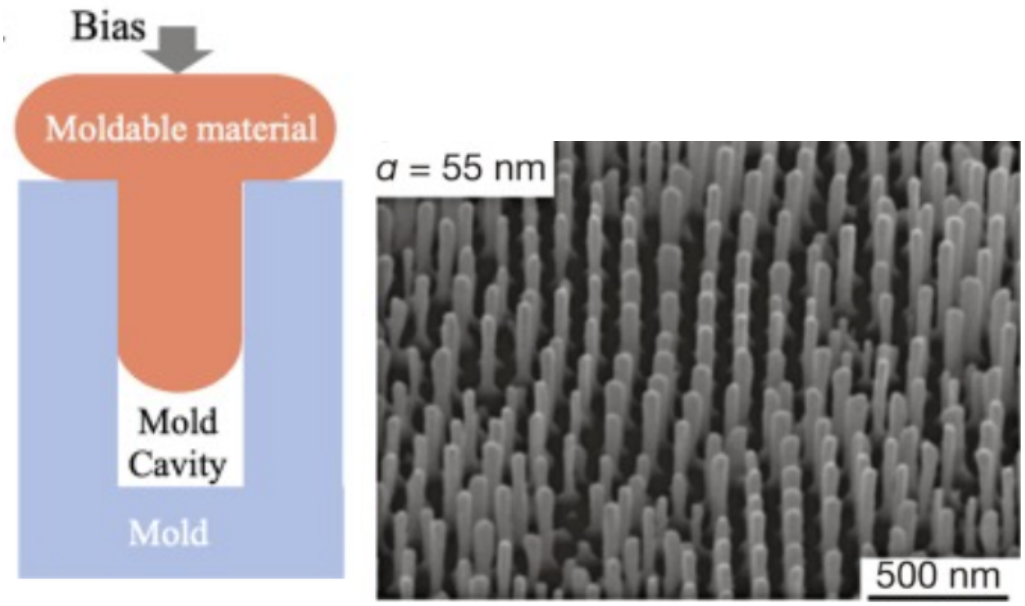

Fig 2. Principle of molding: Left: A moldable material is typically formed under a bias, such as a pressure gradient into a hard mold to fill the mold cavity Right: Using the same molding principle, metallic glass nanorod arrays are molded into mold cavities of 55 nm in diameter.

Image Source: https://doi.org/10.1016/j.pmatsci.2021.100891

Once a moldable feedstock material is introduced, cavity filling is governed primarily by viscous flow and capillary forces. For low viscous materials, capillary forces can dominate infiltration, particularly at small length scales where surface-to-volume ratios are high. For higher-viscosity or near-glassy materials, viscous resistance becomes the limiting factor in cavity filling. However, as feature dimensions shrink toward the nanoscale, capillary effects regain prominence even for relatively viscous systems due to the increasing influence of surface energy.

To aid the molding process, the feedstock may be modified. For amorphous materials(like polymers, plastics, or glass), this is typically achieved by raising the temperature above the glass transition temperature (Tg), the range over which a material transitions from a rigid, brittle glassy state to a rubbery or viscous state with sufficient molecular mobility for flow. Application of dopants to lower the energy required to heat the feedstock to and above Tg can also be pursued.

Considerations such as local temperature control and chemical modification must also be made to ensure that the mold cavity maintains its rigid regime at temperatures well above Tg of the feedstock to avoid contamination and unwanted interaction with it.

3.2 Materials

Material selection for both the feedstock and mold components of the NMNA nanofactory is central to system performance, scalability, and economic viability. The following criteria define the primary engineering constraints.

Abundance.

Candidate materials must be geologically abundant to support eventual large-scale production. A manufacturing platform intended for tonne-scale or greater throughput cannot depend on scarce or strategically limited elements. Abundance directly impacts long-term scalability and cost structure.

Stiffness in the Rigid Regime.

Once solidified, molded components must exhibit high elastic modulus and minimal creep to ensure reliable force transmission and positional stability. Nanoscale mechanical systems are particularly sensitive to deformation, as small strains can translate into significant positional errors. High stiffness is essential.

Dual Feedstock–Mold Capability.

Materials that can function both as moldable feedstock and as rigid mold structures with minimal intermediate modification offer substantial advantages. Such dual-role materials reduce supply chain complexity, simplify thermal compatibility constraints, and enable recursive manufacturing pathways in which a nanofactory can fabricate its own mold components.

Moldability Window (Tg / Viscosity Control).

The material must exhibit a controllable transition into a sufficiently low-viscosity state to allow nanoscale cavity infiltration. This transition should occur within an attainable thermal or chemical regime. Excessively high transition temperatures impose engineering burdens related to energy input, thermal isolation, and material degradation; excessively low transition thresholds risk unintended deformation during assembly or operation. An optimal moldability window therefore balances processability with operational rigidity.

3.3. Deriving and Quantifying Properties.

3.3.1. Elements in top ~10 - 15 crustal and atmospheric abundance

Table 1. Abundance of chemical elements in Earth's (continental) crust, by mass.

Source: Wikipedia.
https://en.wikipedia.org/wiki/Abundance_of_elements_in_Earth%27s_crust

Element	Symbol	Abundance (ppm)	Extraction tonnes/year
oxygen	O	461,000 (46.1%)	10,335,000
silicon	Si	282,000 (28.2%)	7,200,000
aluminium	Al	82,300 (8.23%)	57,600,000
iron	Fe	56,300 (5.63%)	1,150,000,000
calcium	Ca	41,500 (4.15%)	18,000
sodium	Na	23,600 (2.36%)	255,000,000
magnesium	Mg	23,300 (2.33%)	27,700,000
potassium	K	20,900 (2.09%)	53,200,000
titanium	Ti	5,650 (0.565%)	6,600,000
hydrogen	H	1,400 (0.14%)	75,000,000
phosphorus	P	1,050 (0.105%)	226,000,000
manganese	Mn	950 (0.095%)	16,000,000
fluorine	F	585 (0.0585%)	17,000

barium	Ba	425 (0.0425%)	6,000,000
strontium	Sr	370 (0.037%)	350,000

Following this material analysis, by restricting to elements that are abundant in crust, industrially extractable and structurally useful, our primary set would consist of: O, Fe, Na, P, Al, K, Si, Ca, H, Ti, Mg. Additionally, by considering those abundant in the atmosphere by volume[6], the candidates would be: Nitrogen (~78%), Oxygen (~21%), Argon (~0.93%), and Carbon dioxide (~0.04%).

3.3.2. Materials With the Required Stiffness in the Rigid Regime

3.3.2.1. Defining The Actuator Force Envelope (F):

For electrostatic motors:

An electrostatic actuator's force density is given by:

$$P = \frac{1}{2}\varepsilon_0 E^2 \quad \textit{(Eqn 1)}$$

where ***E*** is the electric field, and ε0 is the permittivity of free space (8.854 x 10^{-12} F/m).

Considering that electrostatic actuators will function at much larger μm scales, electric fields at MEMs gaps shall be considered. For MEMS parallel-plate actuators, electric field strengths are on the order of 10^6 to 10^8 V/m. [7]

By using Eqn 1, and assuming ***E*** = 10^8 V/m, we can calculate **the electrostatic pressure,P to be ~4.4MPa.**

Therefore, the material should tolerate 4.4MPa working stress from operating MEMs micro scale.

For thermal expansion nanomotors:

The force generated by a thermally actuated piston depends on the material properties of the actuator and the imposed temperature change. For a thermally expanding element that is mechanically constrained, the resulting force can be derived from linear elasticity as follows:

From Hooke's law:

$$E = \sigma/\epsilon \quad \textit{(Eqn 2)}$$

Where ***E*** is Young's modulus, **σ** is stress and **ϵ** is the strain.

For thermal loading, the strain induced by a temperature change is:

$$\epsilon = \alpha \Delta T \quad \textit{(Eqn 3)}$$

where ***α*** is the coefficient of thermal expansion (K^{-1}) and ***ΔT*** is the temperature change.

Substituting thermal strain into Hooke's law gives the thermally induced stress in a fully constrained element:

$$\sigma = E(\alpha \Delta T) \quad \textit{(Eqn 4)}$$

As the heated rod pushes against an opposing surface, the surface experiences this internal stress,***α*** as a normal force.

Since, normal stress is defined as force per unit area,

$$\sigma = \frac{F}{A} \quad \textit{(Eqn 5)}$$

the force exerted onto a material by thermal piston can be expressed as:

$$F = E(\alpha \Delta T)A \quad \textit{(Eqn 6)}.$$

where ***A*** is the cross-sectional area of the thermally actuated element.

This expression defines the maximum force output of an ideal, fully constrained thermal expansion piston operating within the linear elastic regime.

Regarding piezo electric motors:

Given the authors' intention to employ lead-free piezoelectric materials, particularly $(K,Na)NbO_3$ (potassium sodium niobate) [8], which are less mature and less extensively characterized than conventional lead-based systems such as PZT [9], significant uncertainties remain regarding their practical operating limits. The available literature does not yet provide sufficiently comprehensive data to rigorously define the performance envelope of piezoelectric actuators based on these materials within the scope of the present study.

Accordingly, early iterations of the NMNA nanofactory will prioritize thermal expansion–based actuators for nanoscale operation and electrostatic actuation mechanisms for microscale positioning. With piezo ones considered for later versions after the unknowns are further derisked.

3.3.2.2. Estimated Maximum Stress on Structural Components (σ)

To estimate the maximum stress imposed on representative structural elements, consider a cylindrical rod of length *L* and diameter *D*. The axial stress in the rod under actuator loading is given by:

$$\sigma = \frac{F}{A} \quad \textit{(Eqn 7)}$$

where σ is the normal stress, F is the force applied by the nanoactuator, and A is the cross-sectional area of the rod.

Using Equation 6, the force generated by a fully constrained thermal actuator is:

$$F = E(\alpha \Delta T)A$$

Substituting into the stress expression yields the thermally induced stress:

$$\sigma = E(\alpha \Delta T) \quad \textit{(Eqn 8)}$$

To ensure structural reliability, a safety factor of 3 is applied. The allowable design stress is therefore constrained such that:

$$\sigma_{allowable} \geq 3E\alpha\Delta T \quad \textit{(Eqn 9)}$$

where $\boldsymbol{E}$, is Young's modulus, $\boldsymbol{\alpha}$ is the coefficient of thermal expansion (K^{-1}) and $\boldsymbol{\Delta T}$ is the imposed temperature change

This defines the upper bound of expected operational stress for the selected actuator parameters and establishes a conservative design target for material selection.

Materials with a higher $\sigma_{allowable}$ stress should be considered.

3.3.2.3. Deciding on strain requirements (ε)

To define acceptable strain limits, consider a representative minimum feature size within the system, such as a gear tooth with a height of 10 nm. The engineering strain is given by:

$$\epsilon = \frac{\Delta L}{L} \quad \textit{(Eqn 10)}$$

Where ΔL is the change in length and L original feature dimension.

If the maximum allowable displacement is 0.1 nm on a 10 nm feature, the corresponding strain is:

$$\epsilon = \frac{0.1}{10} = 0.01 = 1\%$$

However, a 1% strain is extremely large for precision nanomechanical components and would result in substantial geometric distortion. To maintain stiffness, dimensional stability, and positional accuracy, operational strains must remain far below this level.

As a general engineering guideline, structural components should operate at less than 10–20% of their failure strain to ensure safe elastic behavior and avoid nonlinear or fracture-dominated regimes. For high-precision nanoscale systems, a more stringent criterion is appropriate.

Accordingly, material selection should ensure that:

$$\epsilon \ll 1\%$$

and ideally within the sub-0.1% regime under peak loading conditions. This constraint preserves structural rigidity and minimizes distortion of nanoscale features during operation.

After evaluating candidate materials against the criteria outlined in Sections 3.3.2.1 through 3.3.2.3, material selection should prioritize those that satisfy the defined mechanical, thermal, and dimensional constraints. Among materials that meet these requirements, preference should be given to those with the highest Young's modulus, as increased stiffness directly reduces elastic strain under load and improves positional stability of nanoscale features.

3.3.3. Fracture resistance.

Fracture toughness is the critical stress intensity factor of a sharp crack where propagation of the crack suddenly becomes rapid and unlimited. It is a material property that quantifies its ability to resist crack propagation and failure under applied stress[10]

One important characteristic for our nanoparts is fracture resistance as cracks in brittle components must be minimized to prevent catastrophic failure of the system.

The stress intensity factor (K) can be stated as[11][12]:

$$K = \sigma\sqrt{\pi a}\, f(a/W) \quad \textit{(Eqn 11)}$$

where *f(a/W)* is a specimen geometry dependent function of the crack length, *a,* and the specimen width, *W*, and σ is the applied stress.

By working backward from our maximum operating stress $\sigma_{allowable}$ from Equation 9 and a maximum flaw size, ***a***, fracture occurs when:

$$K \geq K_{IC}$$

where K_{IC} is material resistance to crack growth.

It is worth it to note that doping and using composites can produce values that greatly exceed the individual fracture toughness of the constituent materials.

Materials with the highest K_{IC} values should be considered.

3.3.4. Reasonable Feedstock Moldability Window (thermal rigidity-viscosity window)

Following mechanical strength and fracture considerations, the thermal moldability window of the feedstock material must be carefully defined. An appropriate balance between rigidity during operation and viscosity during processing is essential for reliable fabrication.

Material selection therefore requires evaluation of two key thermal thresholds:

a. Minimum operational rigidity temperature.

The material must remain mechanically stable and sufficiently rigid at the lowest expected operating temperature, without entering any plastic or viscoelastic regime. If the rigidity threshold is too low, the structure risks dimensional instability or creep under ambient conditions.

b. Moldability temperature (Tg or equivalent softening regime).

The temperature required to transition into a sufficiently low-viscosity state for nanomolding must remain within a practical and controllable range. Excessively high processing temperatures increase thermal noise, structural damage risk, energy consumption, and integration complexity.

An optimal feedstock therefore exhibits a clear separation between its operational rigidity regime and its moldable viscosity regime, allowing reliable structural performance while maintaining feasible processing conditions.

3.4 First-Order Material Selection Heuristic for NMNA Architecture.

No single material simultaneously satisfies all mechanical, thermal, moldability, and fracture requirements defined in the preceding sections. Accordingly, a multi-material or composite architecture is likely necessary, with different materials assigned to specific functional roles based on their inherent strengths.

The following table presents a first-order heuristic for material selection within the NMNA framework. It provides a structured guideline for matching material classes to fabrication stages and operational demands, rather than prescribing a single optimal solution.

Table 2.

Material type	Superiority	Best use-case
Amorphous materials (glass)	Generally well suited for nanomolding feedstock due to isotropy and viscous transition behavior. Especially if they have a reasonably low Tg.	High temperature handling components.
Glass-ceramic *(Starts as glass, is heat treated, undergoes controlled crystallisation and becomes fine crystalline material embedded in glass matrix)*[13]	Higher strength and toughness than glass. Also lower thermal expansion than glass.	High temperature handling components.
Covalent/ionic crystalline ceramics	typically provide higher stiffness and hardness.	Repeated load transmission (rods, gears, pistons, etc.)and high-stress structural components.
Metals or metallic glass	Metals: Provide ductility and crack tolerance via plastic deformation. Metallic glasses: Combine amorphous structure with metallic bonding, offering higher toughness than oxide glasses and potential thermoplastic forming windows.	Components where high crack tolerance matters.
Polymers	Exceptional moldability, low processing temperatures, high strain tolerance, and ease of chemical modification.	unlikely to be primary structural material, however considerations can be made for: Sacrificial molds and templates Compliant or damping components Low-load structural elements Electrical and thermal isolation layers Surface coatings for demolding and friction control Biodegradability and biosafety

3.5. V1 Material Strategy: Polymers as Primary Platform Material

For the first implementation of the NMNA nanofactory, biodegradable polymers are adopted as the primary material. This choice is motivated by its ease of moldability that would enable fabrication of precise geometries of intricate nanomachine parts.
The choice is made deliberately. Known risk categories such as low rigidity and thermal creep may necessitate targeted doping strategies, active mechanical mediation of materials, or, where performance shortfalls are observed experimentally, the introduction of a multi-material architecture in subsequent iterations.

3.6. Preliminary Material Landscape (Scope Limitation).

A comprehensive and fully quantified materials review is beyond the scope of the present study. Detailed thermomechanical characterization, compositional optimization, and process validation will be addressed in subsequent experimental phases. At this stage, material exploration is guided by the mechanical and thermal constraints established in Sections 3.3, 3.4 and later in 6.

3.7 Geometries and Feature Classes.

Nanomolding will be responsible for fabricating the fundamental mechanical elements that constitute nanomachines, as well as nanoparts that can be assembled into larger macro-scale structures.

The most straightforward geometries are simple, planar or quasi-two-dimensional structures commonly encountered in semiconductor nanofabrication, some depicted in Figure 3. These include rods, wires, pillars, raised ridges, tapered needles, and similar features. Such components can be reliably produced using conventional mold-and-press approaches, where viscous feedstock is driven into well-defined cavities and subsequently solidified.

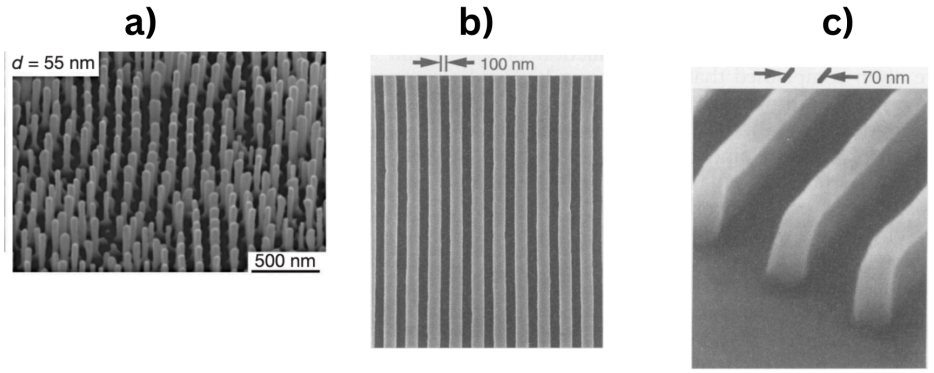

Figure 3. Examples of common nanomolded geometries a) nanorods[14] b) trenches 100 nm wide with a period of 250 nm, formed by compression molding into a PMMA film[15] and c) strips formed by compression molding into a PMMA film

More complex three-dimensional geometries present greater challenges. Structures incorporating undercuts, interlocking features, or embedded microstructures such as gears with shallow teeth,

threaded components (e.g., nuts and bolts), or parts with multiple protrusions that interfere with direct demolding, cannot typically be fabricated using a single-step nanomold process. These geometries require additional strategies to ensure successful formation and release.

Potential workarounds include:

- Sequential or repeatable molding of subcomponents at multiple sites, followed by assembly.
- Post-mold bonding of individually fabricated elements.
- Adaptive modification of the hard mold during processing to direct cavity filling and control viscous flow paths.
- Hybrid fabrication strategies combining molding with secondary machining or assembly steps.

Further refinement of these approaches will be guided by experimental validation and iterative design.

3.8 Resolution Limits

The minimum achievable feature size in nanomolded components is governed by several interacting physical and process-dependent factors including feedstock viscosity, capillary forces within the nanomold, mold geometry, post-mold processing and demolding artifacts.

The target feature size regime for V1 NMNA components is the low-to-mid nanometer scale, nominally 10–50 nm. This range is motivated by two considerations: it sits within the demonstrated capability of existing nanoimprint and nanomolding processes, providing an experimentally grounded starting point, while remaining large enough that continuum mechanical descriptions of material behavior remain substantially valid.

4. Dexterous Nanoassembly

4.1 Minimum Viable Nanoassembly Part Library

A minimal nanomechanical assembly system can be conceptually divided into four primary functional classes: (1) force-generating elements, (2) force transmission and positioning components, (3) a part receiver/donator element and (4) a part joining element.

Force-Generating Elements (Nanomotors)

These components are responsible for introducing mechanical energy into the system. Several actuation mechanisms are considered viable within the NMNA framework, including:

- Thermal expansion actuators, operating via controlled piston displacement within confined chambers [16];
- Electrostatic actuators, utilizing electric-field-induced forces across nanoscale gaps [17];
- Piezoelectric actuators, where applied electric fields induce strain in piezoelectric materials.

The selection of actuation mechanisms will depend on force density requirements, thermal constraints, fabrication complexity, and system integration considerations.

Force Transmission and Positioning Components

Force transmission and positioning elements distribute actuator-generated force throughout the system and direct it to specific locations with controlled motion and mechanical advantage. These components are conceptually inspired by mechanosynthetic architectures and include: Rods, bearings, gears, levers, pistons, springs, etc.

Part receiver/donator elements

These accept molded components from the fabrication stage and present them to the assembly stage. They may also accept already-assembled parts and move them to further assembly stages.

Nanogrippers collecting fabricated parts from cavities post-demolding and transferring them to conveyor platforms is the simplest variation of these components.

Part joining elements

These accept fabricated components and assemble them into larger products. They exist at the nano, micro and macro scales producing products through convergent assembly. Part joining strategies will be covered in section 4.2.

Within the NMNA framework, these elements are realized as nanoscale mechanical proxies rather than atomically precise structures. As such, they may exhibit coarser geometries and larger characteristic dimensions relative to theoretical atomically precise systems, while still preserving the essential mechanical functionality required for deterministic assembly.

4.2 Joining Strategies for Products

Joining strategies within the NMNA framework must operate across multiple length scales. The mechanisms employed vary depending on feature size, load requirements, and structural integration constraints.

Nano and micro scale Joining (nm–μm)

At the nanoscale, joining will combine chemical bonding and mechanical interlocking

Chemical Joining:

- Thermoviscous (sintered) bonding: Local reheating below the crystallization temperature enables viscous flow at contact interfaces, fusing adjacent components without bulk deformation.
- Reactive surface functionalization: Surfaces may incorporate chemically active features (e.g., pores, coatings, or embedded reactants) that form bonds upon contact under thermal or pressure activation.

Mechanical Interlocking:

- Peg-and-socket geometries
- Dovetail-type tapers
- Ball-and-socket features
- Other engineered interlocking profiles

These geometries enable deterministic alignment and load transfer while reducing reliance on purely chemical bonding.

Macroscale Joining (mm–cm and above)

At larger scales, conventional mechanical and materials engineering strategies become feasible. i.e:

- Integrated mechanical fasteners: Components may be molded with built-in threads, grooves, or locking geometries (e.g., bolts, nuts, keyed interfaces).
- Bulk sintering or fusion bonding: Where sufficient surface area is available, thermally assisted sintering can create near-seamless structural integration.
- Fiber-in-matrix architectures.[18]

5. Products

The product space of the NMNA nanofactory is a direct function of manufacturing throughput and assembly complexity. As both improve across successive generations, the range of achievable outputs expands from nanofactory-internal components toward increasingly complex external products. The table below maps each generation of capability to its primary product categories.

Table 3.

Capability / Throughput	Product	Examples
V1: Demonstrating a self-replicating nanomechanical fabricator-assembler	Nanofactory parts	Actuators, sensors, chambers, Stewart platforms, pistons, conveyor mechanisms, pumps, feedstock sorters, etc.
V2: Nanofactory producing a wide variety of useful nanoproducts	Medical nanorobots	Organelle-scale nanomechanical agents with defined mechanical logic and therapeutic capabilities.
	Ultra-high-performance niche nano and micro components	Specialty NEMs, MEMs, engineered nanoparticles, and functional nanosurfaces for industrial and scientific applications
V3: Persistent realisation of useful macro products and recursive nanofactory production	General-purpose high-performance materials	Regeneration-Capable Biodegradable Polymer-based structural components; see Section 6: Components such as clothes, furniture, prefabbed civil infrastructure, electronics, kitchen utensils, medical equipment, etc.
	Edible products	Nutritionally complete products assembled with tuned flavours, textures and nutrient compositions.

5.1 Emergent Macro Properties via Doping and Nanotexturing

A critical observation for the NMNA strategy is that bulk material properties and macro-scale structural properties are not the same thing, and the gap between them is designable. Nature demonstrates this repeatedly. Keratin-based structures such as horn and hoof achieve exceptional impact resistance through a hierarchical fibre-and-matrix architecture assembled from a protein that is relatively unremarkable mechanically at the molecular level.

The NMNA framework is in a position to deliberately engineer the same principle. A polymer that is intrinsically soft at the molecular scale can be nanotextured, surface-patterned, fibre-oriented, porosity-graded, and composite-doped at the nanomolding stage to produce macro-scale structural properties that substantially exceed its bulk values.

6. Nanoshedding and Toxicological Safety

The same properties that make NMNA-fabricated components exceptional i.e: tight nanotextural control, rich doping, and engineered mechanical precision, are precisely what make their uncontrolled environmental release a concern at mass adoption scale. As Drexler articulates in *Radical Abundance*, the long-term vision of nanoassembler-based manufacturing is one in which virtually every material object is produced with nanoscale precision, conferring extraordinary performance at dramatically reduced cost. In that scenario, shedding of nanocomponents from products in everyday use is inevitable, as it is with all materials under mechanical wear, thermal cycling, and environmental exposure.

The specific hazard is biopersistence. Rigid, chemically inert nanoparts released into biological environments cannot be readily broken down by the body's or the greater biosphere's normal clearance machinery. This is exemplified by the growing problem of microplastics polluting much of the environment today[19] and constitutes a foreseeable risk for any high-performance inorganic nanocomponent architecture if not explicitly designed against from the outset.

The guiding safety principle for NMNA products is therefore: **no persistent nano-artefacts**. No component that leaves a manufacturing facility should remain indefinitely in a biological or ecological system. Degradability is a design requirement.

Biodegradable polymers serve as the primary material for end-user nano-products that leave the facility and enter daily human and ecological environments. For this deployment context, biodegradability is added as a first-class material selection criterion alongside the mechanical requirements established in Section 3. Shed fragments from polymer nano-products must enter existing biological degradation pathways rather than accumulating as persistent particulates. Where applicable, some nanofactory components may incorporate polymer building blocks.

6.1 Polymer Candidate Selection Criteria

Material selection for NMNA nano-products follows an analogous framework to that established in Section 3, but with the addition of biological safety as a first-class criterion. Candidate polymers must satisfy most of the following requirements:

Chemical synthesisability from abundant feedstocks. The polymer must be synthesisable from atmospheric and crustal feedstocks (carbon, hydrogen, oxygen, and nitrogen) via thermochemical or electrochemical routes driven purely by energy input. Petroleum-derived feedstocks and bioreactor-dependent synthesis pathways are excluded on radical abundance grounds: a manufacturing platform whose material supply chain is bottlenecked by fossil reserves or biological production capacity has not solved the scarcity problem, it has merely displaced it.

Mechanical performance. Candidate polymers should exhibit high stiffness (Young's modulus), high fracture toughness (K_{IC}), and dimensional stability under operational loading, consistent with the stress and strain limits derived in Section 3.3.2.

Thermal rigidity. The material must remain mechanically stable at expected operating temperatures without entering viscoelastic or flow regimes that would compromise positional accuracy of nanoscale features.

Biodegradability. Shed fragments must enter existing biological or environmental degradation pathways. This is a non-negotiable safety requirement under the no-persistent-nano-artefacts principle established in Section 6.1.

Biocompatibility. The material and its degradation products must not elicit adverse biological responses under expected exposure conditions.

A rigorous quantitative comparison of candidate polymers against these conditions is still needed to narrow the material option space.

6.2 Regenerative Product Architecture

Polymer-based nano-products present an inherent tension: biodegradability is required for safety, but structural degradation during operational life is a functional liability. The NMNA framework resolves this through a regenerative architecture that treats material erosion not as a failure mode but as a managed and correctable process.

Three components work together to achieve this:

Biodegradable bulk material: The product is fabricated from an abundant polymer feedstock with well-characterised biological and environmental degradation pathways. Material shed during normal use is processed by existing ecological or physiological machinery rather than accumulated.

Embedded informatic sensors: Distributed sensing elements integrated into the product structure monitor material integrity in real time, tracking erosion rates, local stress concentrations, and degradation front progression. This gives the product continuous self-knowledge of its own structural health, enabling condition-based maintenance rather than scheduled replacement based on conservative worst-case assumptions

Nanochannel repair network. A network of nanoscale channels running through the product structure serves as a circulatory system for repair material. When sensor data indicates erosion beyond a defined threshold, repair feedstock is delivered through the channel network and deposited at the degradation site. In later iterations, resident nanomachinery within the structures perform active reinforcement, extending functional lifetime autonomously without external intervention. This is akin to the repair mechanism observed in biological tissues[20].

7. Surface Events Control

Stiction and kinetic friction require special consideration as they represent a core risk at this scale as electrostatic, Van der Waals, and hydrogen bonding forces all become significant at nanoscale dimensions [23].

7.1. Anti Stiction

Surfaces separated by as little as 20 nm will almost certainly experience stiction severe enough to impair both the operation and fabrication of components. The following measures are proposed to bring stiction to manageable levels; this list remains subject to revision as experimental data is gathered.

Active Device Design

Electrostatic Charge Dissipation: Conductive paths or conductive coatings are applied to bump stops to prevent electrostatic charge buildup and the attractive forces it generates.
Piezoelectric or Thermal Perturbation: Integrated resistive heaters or piezoelectric actuators provide a brief mechanical impulse to free components that have become adhered.

Innate Physical and Chemical Surface Modification [24]

Physical modification:
Nanoscale Roughening: Controlled increases in surface roughness ensure that only asperity peaks make contact, rather than extended flat areas that would amplify Van der Waals attraction.
Dimples and Bump Stops: Microscopic stand-off structures prevent large flat surfaces from coming into intimate contact, thereby limiting the effective contact area.

Chemical modification:
Self-Assembled Monolayers (SAMs): Low-surface-energy molecular layers covalently bonded to the surface reduce adhesion forces.
Vapor-Phase Lubricants: Lubricant molecules deposited from the vapor phase provide a conformal, low-adhesion coating without requiring liquid-phase processing.
Hydrogen Termination: Passivating dangling bonds with hydrogen reduces surface reactivity and polarity, lowering both Van der Waals and chemical adhesion contributions.

7.2. Artificially Inducing Superlubricity

In atomically precise (AP) mechanosynthetic architectures, superlubricity (the near-elimination of kinetic friction between incommensurate crystalline surfaces) arises naturally from the geometric mismatch between interacting lattices. The NMNA framework operates above the mechanosynthetic limit and therefore cannot rely on structural incommensurability as a friction suppression mechanism. Instead, kinetic friction must be managed through a combination of system-level design choices and active control strategies. The following approaches are proposed.

Slowing down: Reducing component operating velocity directly reduces kinetic energy at contact interfaces and limits frictional heat generation. While this imposes a throughput cost, the tradeoff is necessary in early-stage implementations where surface properties are not fully characterized. Parallelisation across many nanofactory units is the appropriate path to scaling output without increasing per-unit operating speeds.

Dynamic local surface resizing: Integrated thermal or piezoelectric actuators can be used to transiently modulate the local geometry of component surfaces thereby expanding or contracting surface features by sub-nanometer increments to break adhesive contact and reduce the effective

contact area during sliding transitions. This converts a passive stiction problem into an actively managed surface clearance problem.

Nanoscroll-mediated rolling friction: Nanoscrolls are cylindrical structures formed when 2D materials such as graphene wrap around nanoscale particles. By placing them between contacting surfaces, sliding friction can be converted to substantially lower rolling friction[26]. Berman et al. [25] demonstrated that graphene-encapsulated nanodiamond particles spontaneously form nanoscrolls at sliding interfaces, reducing the macroscale coefficient of friction to approximately 0.004 and achieving superlubricity by converting sliding contact into rolling contact while simultaneously presenting an incommensurate surface to the opposing face. Within the NMNA context, the deliberate pre-placement of nanoscroll assemblies at high-contact-frequency interfaces is a candidate strategy for reducing kinetic friction at component interfaces without requiring atomic-scale geometric control.

Fluid and vapor-phase force transmission. Where design constraints permit, replacing solid sliding contact with vapor-phase or fluid-suspended force transmission eliminates the surface-to-surface interaction entirely. Pneumatic or hydraulic coupling within confined nanoscale chambers bypasses the tribological problem at the cost of additional fluid management infrastructure.

Vibration-induced friction reduction: Superlubricity at the atomic-scale can be achieved by introducing an external vibration signal. Tshiprut et al.[27] demonstrated this theoretically, showing that an abrupt dilatancy transition occurs as vibration frequency increases, causing tip-surface separation to grow and frictional resistance to drop.

The strategies above are not mutually exclusive and are expected to be deployed in combination. No single approach eliminates kinetic friction under all operating conditions within the NMNA framework; the practical objective is to reduce friction at high-contact-frequency interfaces to levels that do not limit component lifetime below structurally predicted values. Experimental quantification of the friction coefficients and wear rates achievable under these strategies at the 10–50 nm feature size regime, using the candidate polymer compositions identified in Section 6.1, is a primary priority for the V1 experimental program.

8. Component Stiffness

High rigidity is a prerequisite for reliable force transmission in nanomechanical systems. Afterall, a rod pushes and a rope does not. However, when considering high performance biodegradable polymer candidates such as PEKK, stereochemical-grade PLA, PEA, PEU and high-Tg POx, they exhibit Young's moduli in the 4–15 GPa range. This sits well below the ~1050 GPa of diamond that underpins theoretical AP nanomachine designs, and represents a fundamental performance ceiling that cannot be designed around and only managed.

The 4–15 GPa range figures establish the performance ceiling available to polymer-based nanomechanical components without specifying candidate materials; systematic selection against the criteria of Sections 3 and 6 is reserved for the experimental program.

Three stiffness augmentation strategies are identified as first-order considerations for the V1 experimental program.

Passive material selection. Within the biodegradable polymer candidate space, stiffness varies considerably across subclasses. Those that represent higher-modulus subclasses should be prioritized during candidate narrowing.

Geometric stiffening. Component stiffness is mediated by geometry and not just a material's innate properties. By fabricating a polymer rod shorter than its persistence length[28], it behaves as a rigid element regardless of intrinsic chain flexibility.
Additionally, cross-sectional profiling, such as flanged or I-beam geometries that resist bending moments, and triangular bracing struts that redistribute load, can substantially increase effective structural stiffness beyond what bulk modulus values alone would predict. These are nanomolding-compatible interventions and should be explored in the initial geometry design space.

Stimulation-induced transient rigidity. Passive stiffness may not be the only path to functional force transmission. Myosin offers an instructive analogy: the protein is intrinsically flexible yet performs directed mechanical work by transiently locking its active surfaces into a rigid conformation upon ATP binding, transmitting force during that bound state, then releasing strain through ATP hydrolysis and returning to a low-energy flexible configuration. The force transmission occurs not despite the flexibility but through a controlled, temporary suppression of it. An analogous principle may be applicable in the NMNA context through thermal or electrical stimulation inducing conformational stiffening in an otherwise compliant polymer component, creating a transient rigid state during which force is transmitted, followed by relaxation. Cudjoe et al. demonstrated polymer nanocomposites incorporating cellulose nanocrystals grafted with lower critical solution temperature (LCST) polymers that reversibly switch from a soft state (<1 MPa) to a stiff state (>300 MPa) upon thermal stimulation, with switching reversible across multiple cycles [31]. Electrically triggered stiffness modulation has similarly been demonstrated in shape memory polymer composites doped with conductive nanofillers [32].

9. Performance Limits and Experimental Unknowns

The preceding chapters establish a design framework and first-order parameter space for the NMNA nanofactory. Many physical phenomena and engineering variables have been treated at the level of feasibility estimation rather than rigorous quantification. This is appropriate for a conceptual architecture paper, but each of the following will become a primary experimental constraint as the system moves toward physical realisation:

Friction and wear of nanomechanical components. The tribological behaviour of nanomolded polymer surfaces in sliding or rotating contact is not well characterised at the feature sizes and contact pressures this system will operate under. Surface roughness at the nanomolding resolution limit, combined with the absence of conventional lubricants at this scale, may produce wear rates that limit component lifetime well below structural failure predictions. Experimental measurement of nanoscale friction coefficients and wear rates for the candidate polymer compositions is essential before reliable operational lifetime estimates can be made.

Waste heat considerations. At nanoscale, heat dissipation is rapid due to large surface-to-volume ratios, which is advantageous for cycle frequency, but the thermal gradients induced within a self-contained 100 nm^3 device may be significant relative to component dimensions. Differential

thermal expansion between adjacent components, parasitic heating of non-actuated elements, and cumulative thermal fatigue under repeated cycling are all experimentally unquantified. The thermal isolation strategies implied by the feedstock–mold selectivity discussion in Section 3.5 require experimental validation.

Exact material candidates. Section 3.6 deliberately scopes material selection to feasibility envelopes rather than specific compositions, and the recommendations developed through Chapters 3 and 6 identify candidate classes rather than optimised formulations. Narrowing from material family to specific dopant concentrations, crystallisation protocols, and composite architectures for each functional role requires systematic experimental characterisation.

Throughput and Output Frequency. The undemonstrated material characterization program established in Section 10 is a prerequisite for any rigorous cycle time estimate: mold fill time depends on confined-melt viscosity, solidification time on thermal diffusivity at nanoscale feature dimensions, and demold time on the adhesion forces that the anti-stiction strategies of Section 7.1. Accordingly, operational cycle frequency is treated here as a dependent unknown rather than a derived parameter. Once Tier 1 material characterization is complete, a first-order estimate of cycle frequency can be constructed from the four constituent steps of a single fabrication-assembly cycle (mold fill, solidification, demold, and actuator repositioning)

10. Experimental Path Forward

The preceding chapters establish a design framework and first-order parameter space for the NMNA nanofactory. The transition from framework to physical realization requires a structured experimental program that systematically resolves the unknowns identified in Section 9. This section outlines the proposed research sequence.

The experimental program is organized into three tiers, ordered by logical dependency. Material characterisation must precede fabrication attempts, and fabrication must precede functional assembly validation. However, the three tiers are not strictly sequential as findings at each stage are expected to propagate back upstream, revising material selection criteria, geometric design targets, and actuator specifications iteratively.

Tier 1: Material Characterization. The polymer candidates identified through the criteria of Sections 3 and 6 must be experimentally characterized at nanoscale feature dimensions before fabrication can be reliably attempted. Bulk modulus values drawn from literature are insufficient: mechanical properties at 10–50 nm feature sizes can differ substantially from macroscale measurements due to surface-to-volume effects, chain confinement, and processing-induced microstructural variation. Required measurements include Young's modulus, fracture toughness, glass transition temperature, creep behavior under sustained compressive load, and coefficient of thermal expansion for each candidate composition.

Wear rates and friction coefficients under sliding contact at nanoscale contact pressures are a particular priority, as these directly bound component operational lifetime and inform the friction management strategies outlined in Section 7.

Tier 2: Fabrication Validation. With material properties established, the nanomolding process must be validated for the specific geometries and feature sizes targeted by the NMNA architecture. The central questions are whether cavity filling at 10–50 nm is achievable with the selected feedstock compositions, whether demolding can be accomplished without fracture or geometric distortion, and whether the dimensional fidelity of solidified parts meets the strain tolerance requirements derived in Section 3.3.2.3.

Anti-stiction surface treatments proposed in Section 7.1 will receive their first experimental tests during demolding trials, as stiction between molded part and mold cavity is the primary fabrication failure mode at this scale. Fabrication of the minimal part library defined in Section 4.1 constitutes the completion criterion for this tier.

Tier 3: Functional Assembly Demonstration. The V1 functional target is a minimal proof of concept: one actuator driving one force transmission element to produce a defined displacement at an output point. This demonstration validates the core claim that nanomolded polymer parts can collectively constitute a functional nanomechanical system, and provides the first experimental test of the stiffness augmentation and transient rigidity strategies discussed in Section 8. It also quantifies actuator force output, transmission efficiency, and positional precision under real operating conditions, replacing the analytical estimates of Section 3.3.2 with measured values. Discrepancies between predicted and observed performance at this stage will define the revision targets for V2 material and geometry specifications.

This is the first volumetrically dense polymer nanomechanical system of its kind, with multiple novel solutions operating in concert, and failure modes at each stage are anticipated. The proposed tier-sequencing is designed to ensure that failures are encountered in the right order and that information propagates forward across tiers. Deviations from predicted behavior are treated as design inputs, not terminal outcomes.

11. Conclusion

The central obstacle facing molecular nanotechnology is not theoretical but experimental. The mechanosynthetic architectures articulated by Drexler and others are internally consistent and computationally well-supported, yet they demand angstrom-level atomically precise fabrication as a prerequisite, a capability that remains practically out of reach for first-generation physical realization. The field has lacked a credible intermediate pathway: a framework that is less powerful than full APM but more buildable, and that preserves enough of the functional promise to justify the engineering investment.

This paper proposes the NMNA nanofactory as that pathway. By substituting nanomolding for mechanosynthesis at the fabrication stage and realizing force transmission and assembly elements as nanoscale mechanical proxies rather than atomically precise structures, the framework relocates the experimental challenge from single-atom positioning to nanoscale polymer processing, a domain with

established tooling, characterized materials, and accessible feature size regimes. The result is a self-contained manufacturing architecture that operates above the mechanosynthetic limit while remaining capable of a meaningful subset of its functional outputs.

The contribution of this paper is a design framework, not a demonstration. What has been established here is the parameter space within which a V1 NMNA nanofactory must operate: the mechanical and thermal constraints on material selection, the minimum viable part library for dexterous nanoassembly, the surface force management strategies required at the 10–50 nm scale, the stiffness augmentation approaches available to polymer-based nanomechanical components, and the experimental program through which these parameters will be resolved into physical hardware. The unknowns are named, the failure modes are anticipated, and the research sequence is defined.

The immediate target is modest by the standards of the long-term vision: a single actuator driving a single transmission element, fabricated entirely from nanomolded biodegradable polymer, producing a defined and measurable mechanical output. That demonstration, if achieved, establishes the foundational existence proof for the NMNA architecture, that polymer nanoparts can collectively constitute a functional nanomechanical system. From that foundation, the roadmap toward a productive nanofactory, toward organelle-scale nanomedical agents, and toward the broader transformative potential of molecular manufacturing becomes a question of how volumetrically dense one can pack such nanomachinery.

References.

1. Introduction to Diamond Mechanosynthesis: Robert A. Freitas Jr. and Ralph C. Merkle
2. Nanofabrication through molding: Ze Liu, Naijia Liu, Jan Schroers. Progress in Materials Science, Volume 125, 2022, 100891, ISSN 0079-6425, https://doi.org/10.1016/j.pmatsci.2021.100891 .
3. Engines of Creation: The Coming Era of Nanotechnology: K.Eric Drexler.
4. Schift, Helmut. (2008). Nanoimprint lithography: An old story in modern times? A review. Journal of Vacuum Science & Technology B - J VAC SCI TECHNOL B. 26. 10.1116/1.2890972.
5. K.Eric Drexler, Nanosystems: Molecular Machinery, Manufacturing, and Computation 9780471575184 (ISBN10: 0471575186)
6. Atmospheric Composition, METEO 300: Fundamentals of Atmospheric Science, Penn State, https://courses.ems.psu.edu/meteo300/node/534
7. Microsystem Design, Stephen D. Senturia, Springer Science & Business Media, 2005, ISBN0306476010, 9780306476013.
8. Zhu, LF., Liu, D., Shi, X. *et al.* Ultrahigh piezoelectric performances of (K,Na)NbO_3 based ceramics enabled by structural flexibility and grain orientation. *Nat Commun* 16, 901 (2025). https://doi.org/10.1038/s41467-025-56074-8
9. Lead Zirconate titanate, Wikipedia, https://en.wikipedia.org/wiki/Lead_zirconate_titanate
10. Fracture toughness, Wikipedia, https://en.wikipedia.org/wiki/Fracture_toughness
11. Janssen, M. (Michael) (2004). Fracture mechanics. Zuidema, J. (Jan), Wanhill, R. J. H. (2nd ed.). London: Spon Press. p. 41.

12. Stress intensity factor, wikipedia, https://en.wikipedia.org/wiki/Stress_intensity_factor
13. Examples of glass-ceramics include: Lithium Disilicate ($Li_2Si_2O_5$), Magnesium Aluminosilicate ($MgO–Al_2O_3–SiO_2$, MAS), Cordierite ($Mg_2Al_4Si_5O_{18}$), Apatite–Mullite (Ca–Al–Si–O), Diopside ($CaMgSi_2O_6$), Wollastonite ($CaSiO_3$), Basalt-derived glass–ceramics (Si–Al–Fe–Ca–Mg–O systems), Canasite (K–Ca–Na–Si–F–O), Fluorapatite-based systems (Ca–P–Si–F–O), Leucite ($KAlSi_2O_6$), Enstatite ($MgSiO_3$), Anorthite ($CaAl_2Si_2O_8$), Gehlenite ($Ca_2Al_2SiO_7$), Akermanite ($Ca_2MgSi_2O_7$), Spodumene ($LiAlSi_2O_6$), Phlogopite-based mica glass–ceramics ($KMg_3AlSi_3O_{10}F_2$), Zirconia-toughened glass–ceramics ($ZrO_2–SiO_2$ systems), Nepheline ($NaAlSiO_4$), Forsterite (Mg_2SiO_4), Fresnoite ($Ba_2TiSi_2O_8$)
14. Kumar, G., Tang, H. & Schroers, J. Nanomoulding with amorphous metals. Nature 457, 868–872 (2009). https://doi.org/10.1038/nature07718
15. Chou, Stephen Y., Peter R. Krauss, and Preston J. Renstrom. “Imprint Lithography with 25-Nanometer Resolution.” Science 272, no. 5258 (1996): 85–87. https://doi.org/10.1126/science.272.5258.85
16. K.Eric Drexler, Nanosystems: Molecular Machinery, Manufacturing, and Computation 9780471575184 (ISBN10: 0471575186), Chapter 5.6, Piston displacement in a gas-filled cylinder.
17. K.Eric Drexler, Nanosystems: Molecular Machinery, Manufacturing, and Computation 9780471575184 (ISBN10: 0471575186), Chapter 11.6.4. Electrostatic actuators
18. K.Eric Drexler, Nanosystems: Molecular Machinery, Manufacturing, and Computation 9780471575184 (ISBN10: 0471575186), Chapter 9.3.1
19. Bank, Michael S., ed. 2022. Microplastic in the Environment: Pattern and Process. Cham: Springer. https://doi.org/10.1007/978-3-030-78627-4
20. T.C. Byatt et al, Parallel repair mechanisms in plants and animals, Dis Model Mech (2023) 16 (1): dmm049801. https://doi.org/10.1242/dmm.049801
21. Convergent assembly, Nanotechnology 8 (1997) pages 18-22. https://www.zyvex.com/nanotech/convergent.html
22. Naijia Liu et al. ,Unleashing nanofabrication through thermomechanical nanomolding.Sci. Adv.7,eabi4567(2021).DOI:10.1126/sciadv.abi4567
23. Stiction, Wikipedia, https://en.wikipedia.org/wiki/Stiction
24. Maboudian, R. & Howe, R.T. (1997). "Critical Review: Adhesion in surface micromachining structures." Journal of Vacuum Science & Technology B, 15(1), 1–20. [DOI:10.1116/1.589247](https://doi.org/10.1116/1.589247)
25. Diana Berman et al. ,Macroscale superlubricity enabled by graphene nanoscroll formation.Science348,1118-1122(2015).DOI:10.1126/science.1262024
26. Nano-scrolls may act as a bearing and may also lead to the superlubricity state by changing the friction from sliding to rolling.: https://www.tribonet.org/news/superlubricity-by-means-of-repulsive-van-der-waals-forces/#:~:text=are%20incommensurate.-,Nano%2Dscrolls%20may%20act%20as%20a%20bearing%20and%20may%20also%20lead%20to%20the%20superlubricity%20state%20by%20changing%20the%20friction%20from%20sliding%20to%20rolling.,-Generation%20of%20hydrogen

27. Tshiprut, Filippov & Urbakh (2005): "Tuning diffusion and friction in microscopic contacts by mechanical excitations," Phys. Rev. Lett. 95, 016101. doi:10.1103/PhysRevLett.95.016101
28. Persistence length, Wikipedia, https://en.wikipedia.org/wiki/Persistence_length
29. Marcos Penedo et al. ,Visualizing intracellular nanostructures of living cells by nanoendoscopy-AFM.Sci. Adv.7,eabj4990(2021).DOI:10.1126/sciadv.abj4990
30. Zhang, A., Zheng, G., & Lieber, C. M. (2016). Nanowires: Building Blocks for Nanoscience and Nanotechnology. Springer, https://doi.org/10.1007/978-3-319-41981-7 , Chapter 11.2.3.1, "Strengths and Constraints of Intracellular Measurements", Page 284
31. Cudjoe, E.; Khani, S.; Way, A. E.; Hore, M. J. A.; Maia, J.; Rowan, S. J. Biomimetic Reversible Heat-Stiffening Polymer Nanocomposites. ACS Cent. Sci. 2017, 3 (8), 886– 894, DOI: 10.1021/acscentsci.7b00215
32. Antony, G.J.M., Aruna, S.T., Jarali, C.S. et al. Electrical and thermal stimuli responsive thermoplastic shape memory polymer composites containing rGO, Fe3O4 and rGO–Fe3O4 fillers. Polym. Bull. 78, 6267–6289 (2021). https://doi.org/10.1007/s00289-020-03427-6